STUDY OF MASTER SLIT TRANSMISSION VERSUS EFFECTIVE OPTICAL PULSEWIDTH AND PREBUNCHER AMPLITUDE

M. BAYLAC, J. GRAMES, J.HANSKNECHT, M. POELKER

July 5, 2002

Two short pulse (75 ps) diode lasers were used to emulate effective optical pulse widths from 100 ps to 160 ps by adjusting their relative phase. This was done at optical pulse intensities that produced 499 MHz bunch charges approaching 40% of that required for the G^0 experiment. This was done to provide valuable data regarding the transmission and bunch profile of the resulting electron beam at the master slit aperture of the chopper as a function of optical pulse width and bunching amplitude. In total 6 transmission scans of the bunching amplitude and 46 electron bunch profiles of various conditions were made.

1 Introduction

The G^0 parity experiment scheduled to begin in Fall 2002 in Hall C requires an electron microbunch time structure different than that used for usual end-station operation (499 MHz). Specifically, G^0 requires a microbunch spacing at the 16^{th} sub-harmonic of 499 MHz, or 31.1875 MHz, meaning that only 1 of every 16 RF buckets for Hall C will be filled. Additionally, G^0 requests an average (polarized) electron beam intensity of 40μA at this repetition rate, corresponding to a bunch charge to 1.28 pC, which is an order of magnitude larger than typically delivered.

Prior studies using prototype G^0 lasers indicated that the poor transmission (<40%) through the chopper master slit may corresponded to long optical pulses (150-200 ps FWHM) at the photocathode. Transmission using diode lasers with shorter optical pulses (75 ps FWHM) is generally very high, after bunching. A shorter optical pulse length laser at the G^0 repetition rate is planned for installation. Since this laser is not yet ready for use a test was made to help understand the dependence of transmission on the pulse length for the ultimate G^0 beam with bunch charges as large as attainable, limited by cathode quantum efficiency and laser power. This was done using two diode lasers whose pulses were phased nearly coincident temporally to produce effective optical pulse widths from 100 ps up to 160 ps.

2 Phase I: Tunnel Laser Work (July 1, 0800-1230)

The test required installing a second 499 MHz diode laser (POLOG#16636) matched similarly to one already installed in order to achieve both the short optical pulse length and wavelength near 770 nm to take advantage of the peak quantum efficiency, thus highest bunch charge. This was done and two lasers, called throughout this report as "laser A" and "laser B", were configured in the tunnel. The co-linearity of the two optical paths were checked finally using a Spiricon imaging system located at a distance to, and mimicing, the photocathode. The FWHM optical beam sizes were measured at this location and the results are laser A= 475 μm and laser B=510 μm, within 10% of one another.

Because of the requirement that the two laser pulses overlap temporally the RF cable length of the B laser was changed so that its pulse timing was equivalent to the A laser. This was measured using a fast photodiode and digital scope used for optical pulse measurements. In addition to the usual 3-laser phase shifting RF controls, a remotely controlled mechanical phase shifter was installed on the B laser, however, it was ultimately not needed in the test.

3 Phase II: Beam Restoration (July 1, 1230 - 1800)

Following the laser work scans of the photocathode quantum efficiency versus laser spot location were done to recalibrate the laser location on the photocathode and to compare the coincidence of both lasers. To be expeditious the tunnel was locked up and we began the scans remotely. Unfortunately an unrelated maintenance issue of the steering mirror gear shaft delayed this work twice, requiring two accesses. Additionally, the RF group made an access to perform measurements of the prebuncher cavity. Ultimately, the photocathode scans were made (POLOG#16642) and the coordinates (x=1300, y=1580) of highest quantum efficiency location determined.

Finally, the gun high voltage was restored and the A laser was used to tune the beam to Faraday Cup #1 (FC1) through the Hall A 60° chopping aperture. The Wien angle was set to 0° to remove its role in the modeling and the beam was optimized in CW mode to minimize interception on transverse beam size apertures A1 & A2. Next, the B laser was used to determine the quality of beam orbit coincidence. The B laser orbit differed from the A laser by < 1 mm throughout. Remote laser table mirrors were used iteratively steering the B beam toward the A beam and then the A beam toward the B beam in a way that maximized the transmission of both and made the two coincident (POLOG#16647). As a final mark, the B orbit relative to the A orbit is shown in Figure 1.

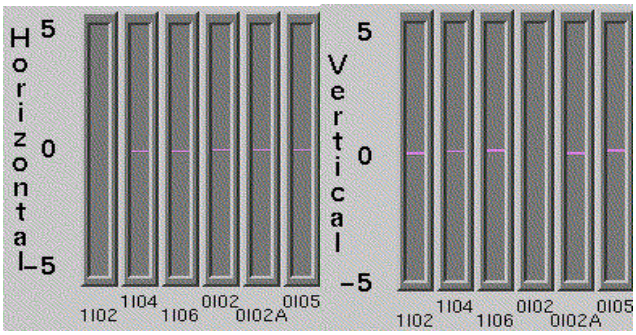

Figure 1. The A laser generated beam orbit is shown with respect to the B laser generated orbit in CW mode after iteratively steering one toward the other to maximize transmission and minimize orbit difference. Vertical units are in millimeters. 1I02-0I02A are upstream of the chopper, 0I05 is directly downstream.

4 Phase III: Initial Beam Tests (July 1, 1800 - 2400)

This portion of the testing primarily involved electron bunch profile scans to determine and properly locate the central phase location of the A laser, B laser, and prebuncher. It also included measurement of the bunch profile at low current and minor adjustment of the seed laser power to shape the profiles to be more similar to one another. Afterwards the longitudinal bunch profiles of the A beam and B beam were made at a series of beam intensities (10 to 170 μA) individually and then in superposition (20 to 274 μA). The list of electron longitudinal profiles measured for this portion of the test are given in Appendix A.

Initial low intensity bunch profiles (10 μA/laser) of the A and B beams are shown in Figure 2. The seed laser power was adjusted so to lengthen the A laser pulse and shorten the B laser pulse. The resultant pulse shapes were then measured again at low current and the central phase locations of the A and B laser are determined from these scans, shown in Figure 3.

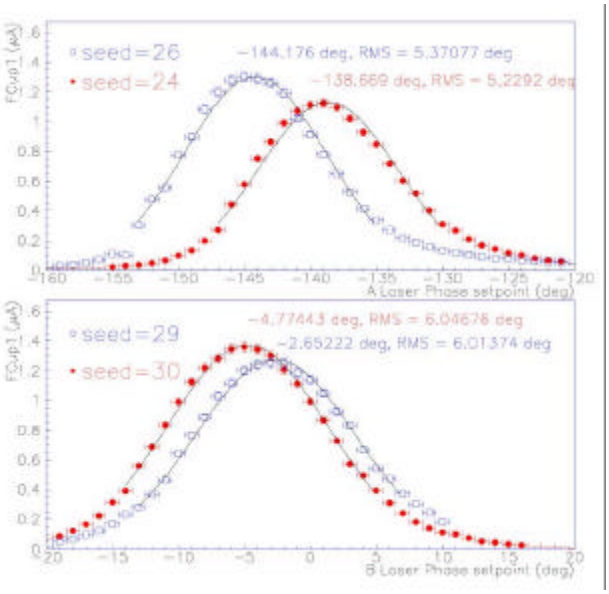

Figure 2. The diode laser seed currents were adjusted to make the pulse widths of the two lasers more similar. The upper plot shows that the A laser pulse width was increased (seed from 24 to 26) 2.6% while the lower plot shows that the B laser pulse width was decreased (seed from 30 to 29) 0.7%. Varying the seed current further impacted the total laser power unacceptably. Ultimately, the two laser pulse widths are within 10% of one another.

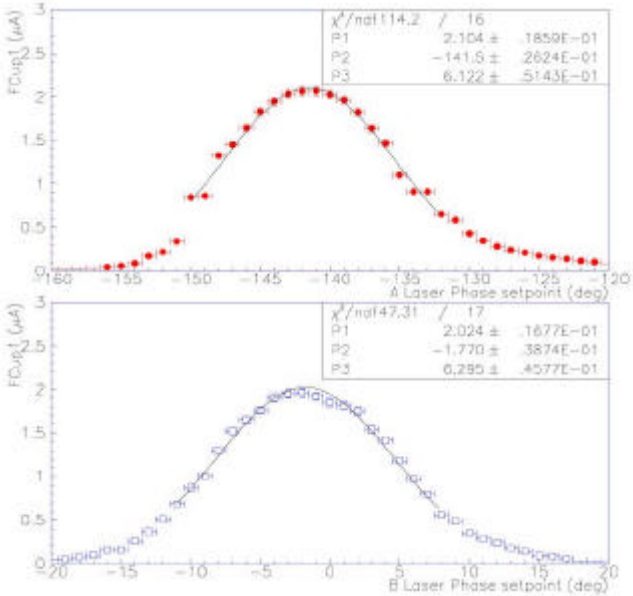

Figure 3. Profiles of the two diode laser generated beams at low intensity (10 μA) yield the central phase which passes through the 10° chopping aperture and the effective width of the bunch (convoluted with the aperture size). The measured FWHM of the A bunch is 75 ps and the B bunch is 77 ps.

Next the longitudinal intensity profiles of the A and B electron bunches were measured individually and in superposition (POLOG#16652) with the configurations described in Table 1. This was done without the use of the prebuncher over the range 0.02 to 0.55 pC. The purpose of this measurement is to indicate the facility of emulating a single bunch by superposing two bunches and to provide data at various bunch charges for quantitative consideration (calculation or modeling). Profiles of the individual (single laser) bunches are shown in Figure 4.

Run (#)	9	10	11	12	13	14	15	16	17	18	19	20
A (μA)	171	173	171	0	116	116	50	50	0	0	10	10
B (μA)	114	0	0	114	0	114	51	0	51	10	0	10
A+B (μA)	274	173	171	114	116	221	101	50	51	10	10	20
Q_{bunch} (pC)	0.549	0.347	0.343	0.228	0.232	0.443	0.202	0.100	0.102	0.020	0.020	0.040

Table 1. A list of the A & B laser generated bunch conditions is shown. To investigate the interaction of the two bunches near one another in time and space and at different beam intensities bunching was not yet employed.

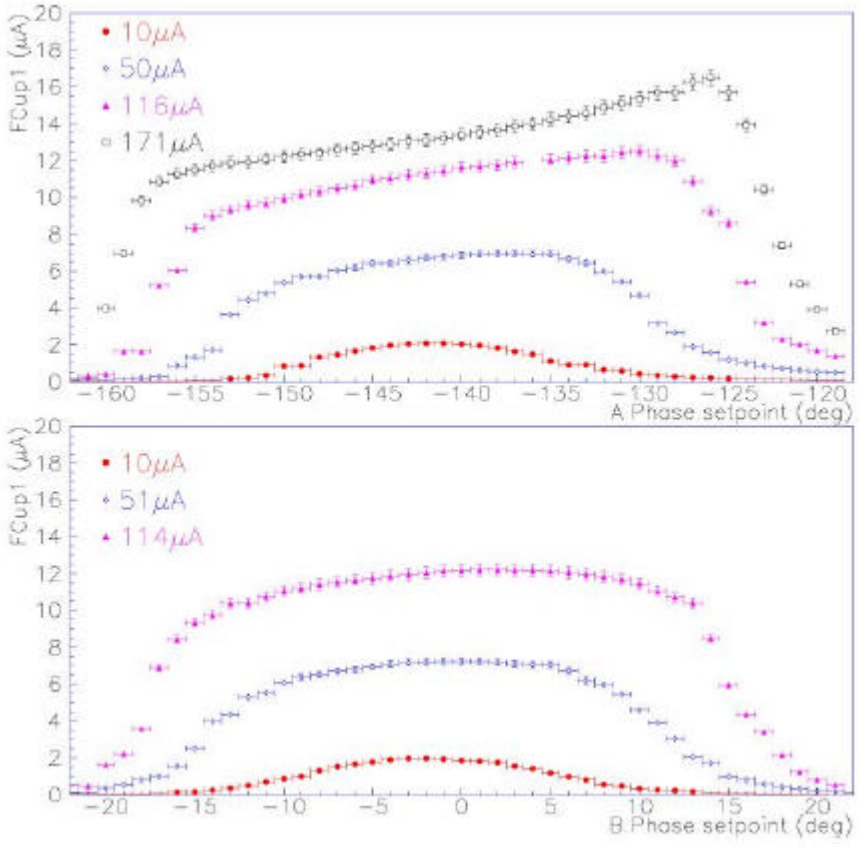

Figure 4. The longitudinal electron bunch profiles for the individual A & B lasers are shown. In each profile the head of the bunch is at the more positive phase.

Before beginning transmission measurements the prebuncher was phased for zero-crossing. This was done, as usual, by turning the laser RF off to obtain a DC beam of a few microamps and then turning the prebuncher on at a moderate value to obtain a 1497 MHz bunched beam which carries the phase of the prebuncher. Using the chopping apertures slits, either fully open (60° at 499 MHz) or at the bunch profile measurement width (10° at 499 MHz), a phase scan cross-calibrates the prebuncher phase to the laser phase (as set by the 10° aperture), all at low current. Next, we verified the phase direction of the A laser, B laser, and prebuncher using the 0I04 chopping viewer. We found that in all cases a positive increment to the phase of either of the devices rotates the electron bunch in the same direction (in the case of the 0I04 viewer, clockwise).

Unfortunately, upon backing out of this procedure we found that the A laser was responding unusually. The symptoms were that the A bunch phase appeared to have increased by about 45 degrees, a large amount of DC beam (DC light) was apparent, and the laser power dropped by about 75%. Occasionally, but briefly, the laser would appear to lock-in at the right phase and provide the usually good profile. We believed the A laser had failed. With all of our resources exhausted and only one laser available we postponed our troubleshooting and effort until the next shift and left the B laser available for Operations for the evening for other testing (POLOG#16650).

5 Phase IV: Troubleshooting the A Laser (July 2, 0730 - 0930)

The A laser was investigated the following morning (POLOG#16657), however, whatever had plagued its operation the night before did no longer. The laser power, pulse structure, and timing were all functioning well and within specification. The seed laser controls were exercised and found to have no meaningful sensitivity on the laser phase. Some RF connectors at the amplifiers in the 3-laser rack were found to be only hand tight and were tightened further, however, the A laser was operating well already. Having exhausted the reasonable possibilities we stopped investigating and prepared the lasers for operation. No laser problem occurred during the remainder of the test.

6 Phase V: Transmission and Electron Bunch Profile Scans (July 2, 1200 - 1600)

Beam testing resumed in the afternoon picking up where we had left off the previous evening. First, the bunch profiles were checked to verify the A & B laser were coincident and the prebuncher at zero-crossing at low beam intensity (20 μA per profile) for three bunch separations ($\delta t = 0°, 12°, 16°$). The scans are shown in Figure 5.

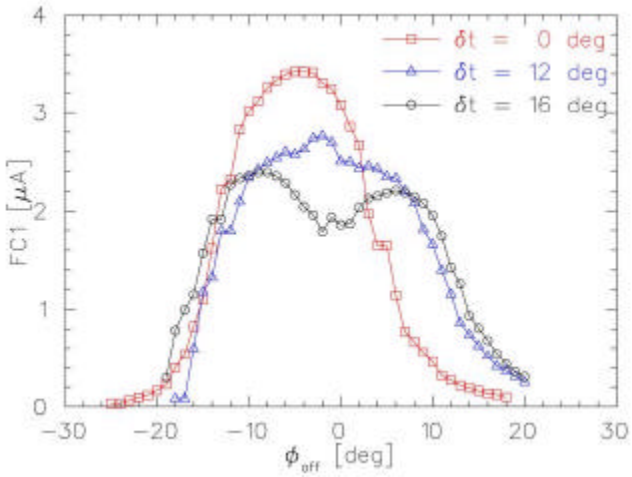

Figure 5. Electron bunch profiles for the three cases of laser separation are shown. The FWHM bunch lengths estimated from the plot for increasing laser pulse separation are 100 ps, 139 ps, and 161 ps, respectively. The single laser bunch length is 75 ps, providing an estimate of how well two bunches overlap for the $\delta t = 0°$ case.

Transmission and bunch profile measurements at three laser pulse separations followed and are described in Table 2. The list of electron longitudinal profiles measured for this portion of the test are given in Appendix B. Results of the transmission tests are shown in Figure 6 and the data tables are listed in Appendix C.

Scan [#]	A intensity [μA]	B intensity [μA]	Total [μA]	δt [deg]	FWHM [ps]	Prebuncher [deg]
1	Unknown	Unknown	263	0	100	-150
2	Unknown	Unknown	258	0	100	-140
3	110	99	210	12	139	-145
4	76	76	152	12	139	-145
5	76	76	152	16	161	-145
6	108	107	205	16	161	-145

Table 2. Prebuncher amplitude scans for different beam intensities as a function of pulse separation are described.

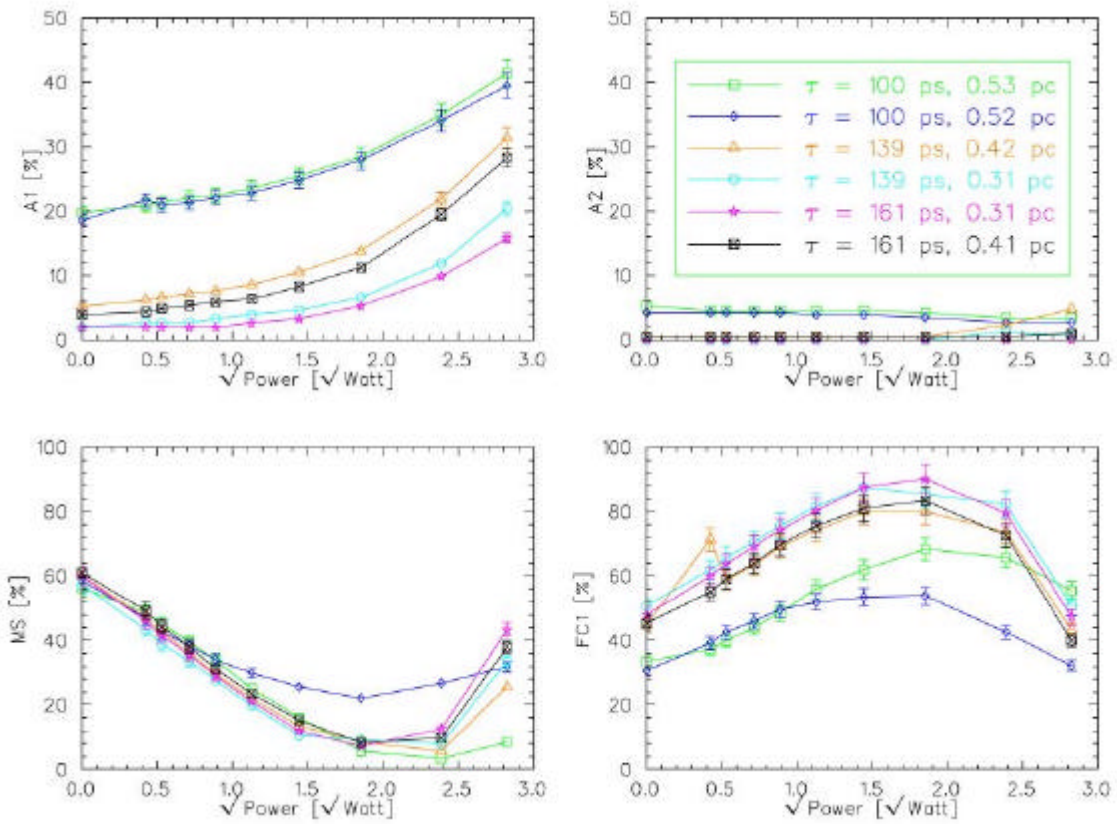

Figure 6. Transmission studies of the A1, A2, and MS apertures and Faraday cup #1 were made as a function of the prebuncher setpoint (Off to 33 dBm) for two different bunch charges at each of the three laser pulse separations. A separate measurement of prebunching power as a function of setpoint was made and the results shown above are plotted versus the square root of the applied power, in terms of un-normalized bunching field gradient.

The result of the transmission scans indicates the optimum prebuncher setpoint is 3.43 Watt. The FC1 transmission for the six cases at this optimum are presented in Figure 7. For the two longer bunch lengths the trend is that a) the lower bunch charge or the longer bunch length has higher transmission. Unfortunately, the shortest bunch length was not tested with similar bunch charge. For the case $\delta t=0°$ the two datum have nearly identical bunch. The difference in the transmission is that the prebuncher phase was adjusted by 10° (1497 MHz). See Table 2 for details.

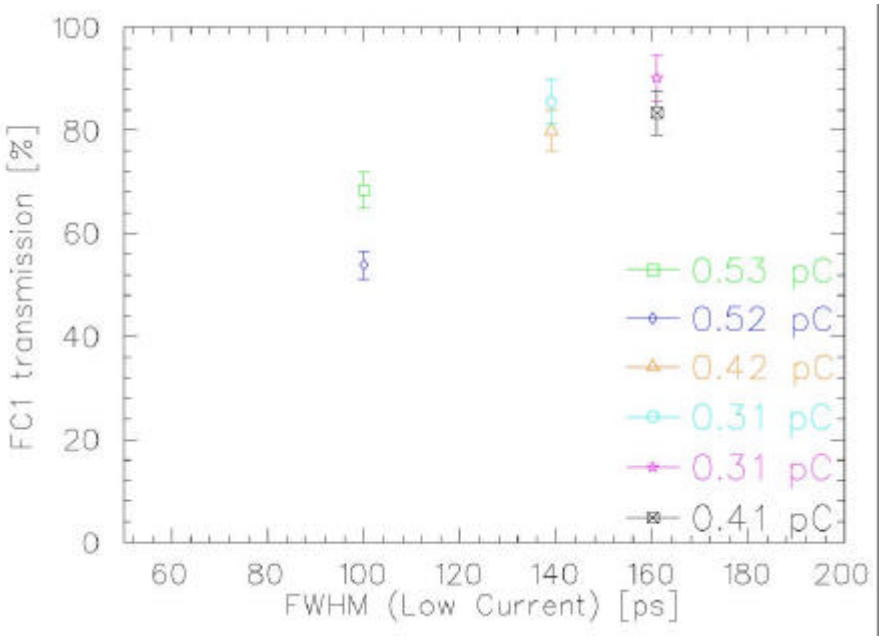

Figure 7. The FC1 transmission at the apparent optimum prebuncher setpoint of 29 dBm (3.43 Watts) for the six prebuncher scans is shown as a function of the FWHM measured (low current) bunchlength.

For the remaining longitudinal bunch profiles please refer to Appendix B for conditions and to the referenced data files which are stored on the Operations cluster.

7 Conclusions

In summary, we completed a series of measurements which should provide some insight into the longitudinal evolution of the bunch from the gun to chopping apertures for various initial conditions and prebunching. We measured the longitudinal bunch profile for single electron bunches from 0.02 to 0.35 pC and for combined electron bunches from 0.04 to 0.55 pC with initial bunch lengths of 100 ps. We then measured the transmission of the relevant apertures with three pulse separations (0°, 12°, 16° at 499 MHz), corresponding to three FWHM initial bunch lengths of 100 ps, 139 ps, and 161 ps, as a function of the zero-crossing prebuncher amplitude. We found that the prebunching amplitude corresponding to 3.43 Watts appeared to result with a minimum in interception at the 60° chopping aperture. We measured the electron bunch profile for all of the stated conditions, as well. Finally, we found that for this set of measurements there is an indication that the lower bunch charge has higher transmission (not surprising) and that the longer bunch charge has higher transmission. Of course, these are simply first tests which require more systematic study. Such a study is planned in the near term at bunch charges more comparable with that needed for G^0.

8 Acknowledgements

We would like to thank A. Bell, J. Benesch, C. Hovater, G. Lahti, J. Musson, and M. Wissmann for putting the prebuncher into a known, usable mode for this test and B. Yunn for suggesting the modeled need to do so.

9 Appendices

The data in the appendices are stored on the operations cluster in */cs/op/lib/xtract/data/g0test*. Data files are column format with the first row of the file indicating the name of each column of data. Please copy data files if editing.

Appendix A: July 1, 2002 (Runs 01-22)

Run#	Slit	A laser	B laser	Prebuncher	Comment
Run01	-1	-140 to -120 @70	N/A	N/A	Test scan A(6uA)
Run02	-1	-160 to -120 @70	N/A	N/A	Test scan A(6uA)
Run03	-1	-180 to -100 @70	N/A	N/A	Test scan A(6uA)
Run04	60	-180 to -100 @70	N/A	N/A	No Beam A(6uA)
Run05	60	-180 to -100 @70	N/A	N/A	A&B Home/Reset (6uA)
Run06	60	N/A	-40 to 30 @70	N/A	Test Scan B(6uA)
Run07	60	-160 to -120 @78	N/A	N/A	A(6uA) seed from 24 to 26
Run08	60	N/A	-30 to 10 @	N/A	B(6uA) seed from 30 to 29
Run09	60	-164 to -119 @600	-23 to 22 @600	N/A	A+B=274uA
Run10	60	-164 to -119 @600	N/A	N/A	A(173uA)
Run11	60	-164 to -119 @600	N/A	N/A	A(171uA)
Run12	60	N/A	-23 to 22 @600	N/A	B(114uA)
Run13	60	-164 to -119 @380	N/A	N/A	A(116uA)
Run14	60	-164 to -119 @380	-23 to 22 @600	N/A	A+B=221uA
Run15	60	-164 to -119 @235	-23 to 22 @290	N/A	A+B=101uA
Run16	60	-164 to -119 @235	N/A	N/A	A(50uA)
Run17	60	N/A	-23 to 22 @290	N/A	B(51uA)
Run18	60	N/A	-23 to 22 @110	N/A	B(10uA)
Run19	60	-164 to -119 @110	N/A	N/A	A(10uA)
Run20	60	-164 to -119 @110	-23 to 22 @110	N/A	A+B=(20uA)
Run21	-1	N/A	N/A	-241 to -110 @33	Best=-165 (laser RF off)
Run22	60	N/A	N/A	-190 to -140	B&C=closed, laser RF off

Appendix B: July 2, 2002 (Runs 23 to 46)

Run#	Slit	A laser	B laser	Prebuncher	Comment
ϕ=0°					
Run23	60	-164 to -119	N/A	N/A	Test scan A(10uA)
Run24	60	N/A	-23 to 22	N/A	Test scan B(10uA)
Run25	60	-137	N/A	-195 to -135	Test scan PB+A(10uA)
Run26	-1	-137	N/A	-195 to -135	Test scan PB+A(10uA)
Run27	-1	-137	N/A	-195 to -105	Test scan PB+A(10uA)
Run28	-1	N/A	-3	-195 to -105	Test scan PB+B(10uA)
Run29	-1	-137	-3	-195 to -105	PB & A+B=260uA
Run30	-1	-167 to -107	-33 to 27	-195 to -105	PB & A+B=260uA
Run31	-1	N/A	N/A	N/A	Bad run
Run32	-1	-167 to -107	-33 to 27	N/A	A+B=260uA
Run33	60	-137 to -107 @378	N/A	N/A	A(111uA)
Run34	60	N/A	-33 to 27 @600	N/A	B(110uA)
ϕ=12°					
Run35	60	-163 to -123 @110	-17 to 23 @117	N/A	A(10uA)+B(10uA)
Run36	60	-163 to -123	-17 to 23	N/A	A(100uA)+B(100uA)
Run37	60	N/A	N/A	N/A	Accidental C1 scan
Run38	*60*	*-163 to -123*	*-17 to 23*	*-180 to -120 @29*	
ϕ=16°					
Run39	60	-165 to -125 @372	-15 to 25 @600	N/A	A(108uA)+B(97uA)=203uA
Run40	60	-165 to -125 @300	-15 to 25 @400	N/A	A(76uA)+B(76uA)=148uA
Run41	60	-165 to -125 @110	-15 to 25 @117	N/A	A(10uA)+B(10uA)=20uA
Run42	60	-165 to -125 @255	-15 to 25 @290	N/A	A(51uA)+B(50uA)=101uA
Run43	60	-165 to -145 @255	-15 to 25 @290	-205 to -85 @29	A(51uA)+B(50uA)=100uA
Run44	60	-165 to -145 @110	-15 to 25 @117	-205 to -85 @29	A(10uA)+B(10uA)=20uA
Run45	60	-165 to -145 @300	-15 to 25 @400	-205 to -85 @29	A(73uA)+B(73uA)=145uA
Run46	60	-165 to -145 @372	-15 to 25 @600	-205 to -85 @29	A(106uA)+B(94uA)=198uA

Appendix C: Prebuncher Scan Data

Scan #1, Pcup=263 μA, δt=0°, ϕ_{pb} = -150°

Prebuncher [dBm]	Prebuncher [Watt]	A1 [mA]	A2 [mA]	MS [mA]	FC1 [mA]
Off					
17	0.18	55	12	128	98
19	0.28	56	12	119	105
21	0.51	58	12	104	116
23	0.79	59	12	89	128
25	1.27	62	12	66	167
27	2.08	67	12	42	163
29	3.43	75	11	15	180
31	5.70	92	9	9	173
33	7.97	109	8	22	146

Scan #2, Pcup=258 μA, δt=0°, ϕ_{pb} = -140°

Prebuncher [dBm]	Prebuncher [Watt]	A1 [mA]	A2 [mA]	MS [mA]	FC1 [mA]
Off	0.00	48	11	151	79
17	0.18	56	11	121	101
19	0.28	54	11	110	110
21	0.51	55	11	99	119
23	0.79	57	11	88	128
25	1.27	59	10	77	134
27	2.08	64	10	66	138
29	3.43	72	9	57	139
31	5.70	88	7	69	110
33	7.97	102	7	82	83

Scan #3, Pcup=210 μA, δt=12°, ϕ_{pb} = -145°

Prebuncher [dBm]	Prebuncher [Watt]	A1 [mA]	A2 [mA]	MS [mA]	FC1 [mA]
Off	0.00	11	1	126	94
17	0.18	13	1	99	150
19	0.28	14	1	89	123
21	0.51	15	1	76	133
23	0.79	16	1	62	145
25	1.27	18	1	46	156
27	2.08	22	1	28	168
29	3.43	29	1	18	168
31	5.70	46	5	12	155

33	7.97	66	10	54	91

Scan #4, Pcup=152 μA, δt=12°, ϕ_{pb} = -145°

Prebuncher [dBm]	**Prebuncher [Watt]**	**A1 [mA]**	**A2 [mA]**	**MS [mA]**	**FC1 [mA]**
Off	0.00	3	0	87	77
17	0.18	4	0	66	94
19	0.28	4	0	59	100
21	0.51	4	0	51	107
23	0.79	5	0	42	115
25	1.27	6	0	30	124
27	2.08	7	0	16	133
29	3.43	10	0	14	130
31	5.70	18	2	12	125
33	7.97	31	1	51	77

Scan #5, Pcup=152 μA, δt=16°, ϕ_{pb} = -145°

Prebuncher [dBm]	**Prebuncher [Watt]**	**A1 [mA]**	**A2 [mA]**	**MS [mA]**	**FC1 [mA]**
Off	0.00	3	0	91	73
17	0.18	3	0	70	91
19	0.28	3	0	63	97
21	0.51	3	0	54	105
23	0.79	3	0	44	113
25	1.27	4	0	32	122
27	2.08	5	0	18	133
29	3.43	8	0	11	137
31	5.70	15	0	19	121
33	7.97	24	0	66	72

Scan #6, Pcup=205 μA, δt=16°, ϕ_{pb} = -145°

Prebuncher [dBm]	**Prebuncher [Watt]**	**A1 [mA]**	**A2 [mA]**	**MS [mA]**	**FC1 [mA]**
Off	0.00	8	1	125	93
17	0.18	9	1	101	113
19	0.28	10	1	91	121
21	0.51	11	1	78	131
23	0.79	12	1	64	143
25	1.27	13	1	48	155
27	2.08	17	1	31	166
29	3.43	23	1	17	171
31	5.70	40	1	20	143

33	7.97	58	2	78	82